J. Dairy Sci. 105
https://doi.org/10.3168/jds.2021-21452
© 2022, The Authors. Published by Elsevier Inc. and Fass Inc. on behalf of the American Dairy Science Association®.
This is an open access article under the CC BY license (http://creativecommons.org/licenses/by/4.0/).

Investigation of breakage behavior and its effects on spray-dried agglomerated whey protein-lactose powders: Effect of protein and lactose contents

Jie Han,[1,2] John Fitzpatrick,[2] Kevin Cronin,[2] Valentyn Maidannyk,[1] and Song Miao[1]*
[1]Teagasc Food Research Centre, Moorepark, Fermoy, Co. Cork, Ireland P61 C996
[2]Process & Chemical Engineering, School of Engineering, University College Cork, Cork, Ireland T12 CY82

ABSTRACT

Particle breakage of dairy powders occurs easily during many processes, reducing the powder functionality. The characteristics of particles and the applied stress from processing conditions on the particles are 2 main factors that can be manipulated to reduce breakage. In this study, we explored the effect of whey protein and lactose contents on dynamic breakage in agglomerated whey protein-lactose powders to provide useful information, in terms of particle characteristics, for controlling unwanted dairy powder breakage. A series of model agglomerates with different whey protein:lactose ratios were produced under the same spray-drying conditions, through a pilot plant trial. We evaluated physical characteristics, composition, and structure of samples; analyzed dynamic breakage under different mechanical stresses; and investigated the rehydration and water adsorption properties of model powders before and after breakage. The particle size and irregularity of agglomerates with more lactose was significantly higher than of samples that contained more protein. This resulted in higher particle breakage during dynamic breakage for samples with more lactose. The breakage of agglomerates was affected by the moisture content of powders and fatigue, where particle breakage happens when mechanical loads, lower than the strength of particles, occur multiple times. Breakage changed the morphology and surface composition of particles and decreased particle size. It also decreased the dispersibility of powders and increased the wetting time of wettable samples but decreased the wetting time of powders with poor wettability. Breakage accelerated time-dependent crystallization and decreased the crystallization temperature but did not affect the glass transition temperature of samples. Thus, under the same drying conditions, composition of powders significantly affected breakage, mainly by altering the physical properties of their particles, which resulted in deteriorated functionality.

Key words: spray-dried agglomerated whey protein-lactose powders, particle size, particle structure, dynamic breakage, rehydration properties

INTRODUCTION

Dairy powders provide a good form for stable and convenient preservation and transportation of dairy ingredients. However, particle breakage of dairy powders happens easily during the production, transportation, and handling after spray drying and agglomeration, especially for agglomerated powders. Breakage will occur when particles are subjected to mechanical stresses, such as shear, impact, and compression, due to collisions of particles with static container walls and other particles (Kotzur et al., 2018). Dairy powder breakage has been found to occur during in-plant transportation by a bucket elevator or pneumatic conveying, dry mixing, vibration, and compression (Yan and Barbosa-Cánovas, 2001a,b; Boiarkina et al., 2016; Hazlett et al., 2020; Zhang et al., 2020).

Particle breakage causes significant deterioration in the properties and functionalities of dairy powders. It decreases the porosity and particle size of dairy powders and increases their surface area and density (Hanley, 2011; Boiarkina et al., 2016; Han et al., 2020; Hazlett et al., 2020; Zhang et al., 2020). In addition, the surface composition and particle morphology of dairy powders change after breakage. These changes reduce the rehydration properties of dairy powders, such as infant milk formula (**IMF**), fat-filled milk powder, whey protein isolate (**WPI**), and whole milk powder (Han et al., 2020; Hazlett et al., 2020; Zhang et al., 2020). Breakage also accelerates water adsorption rates and time-dependent crystallization and increases the final water content of IMF. These phenomena necessitate stricter requirements for the powder storage environ-

Received October 19, 2021.
Accepted June 10, 2022.
*Corresponding author: Song.Miao@teagasc.ie

ment to prevent caking or other deterioration, such as lower storage water activity ($\mathbf{a_W}$) and temperature.

Based on particle breakage research in other industries, the characteristics of particles and the force applied on particles from processing conditions are 2 main factors that determine the response of particles to the given loading condition (Yan and Barbosa-Cánovas, 2001a; Petukhov and Kalman, 2004; Lu et al., 2014; Kotzur et al., 2018). Therefore, these 2 factors can be manipulated to reduce unwanted dairy powder breakage. The processing conditions, such as parameters during dry mixing, vibration, and transportation by pneumatic conveying, play a fundamental role in the occurrence of dairy powder breakage. Increased breakage of instant milk powders was found as the tapping number increased during the tapping test (Yan and Barbosa-Cánovas, 2001a). Hanley (2011) reported that dilute-phase pneumatic conveying caused more breakage of IMF than dense-phase pneumatic conveying because it required a higher superficial air velocity, which resulted in higher-energy collisions against the bends (Kalman, 1999).

In addition to the applied forces from processing conditions, powder breakage depends on the powder's characteristics, including its physical properties (morphology, particle size, particle size distribution, powder porosity, and densities) and composition (Han et al., 2021b). Based on previous research that compared the breakage of 15 dairy powders, particle size, porosity, and particle structure were the most important particle physical properties that influenced breakage (Han et al., 2021c). Regarding the effect of powder composition, limited research has been done on comparing different commercial dairy powders. It is thought that fat might increase the compressibility of dairy powders because fat liquefaction can soften powders, resulting in the easy deformation of particles (Yan and Barbosa-Cánovas, 1997; Rennie et al., 1999). Hanley et al. (2011) explored the breakage of 4 types of IMF with the same particle size range but different protein-to-fat ratios during pneumatic conveying and found more breakage for 2 lower-protein IMF. However, the differences in spray-drying parameters between these compared samples were not considered and these parameters would influence the physical properties of particles and, in turn, affect their breakage behavior. Moreover, protein and lactose are the most common basic ingredients in milk powders; therefore, investigating the effect of the relative content of these 2 components on the breakage of dairy powders will provide useful information for controlling breakage.

In this study, we prepared a series of agglomerated WPI-lactose model powders by a 3-stage spray dryer under the same spray-drying conditions to investigate the effect of whey protein and lactose content on the breakage of model powders and the effect of that breakage on powder properties. Two types of breakage were considered to investigate the effect of fatigue, where particle breakage happen when mechanical loads, lower than the strength of particles, occur multiple times: dynamic breakage under different mechanical stresses in a venturi feeder, which mimics pneumatic conveying, and breakage under repeated laboratory-scale dilute-phase pneumatic conveying. Then, we investigated the effect of breakage on the rehydration and water adsorption properties of the model powders because these 2 parameters decline the most in powders after breakage.

MATERIALS AND METHODS

Materials

Whey protein isolate (Provon 295, protein content 88.59%; ash content 2.66%; moisture content 4.59%) and lactose (LAFB Vegetarian Lactose, lactose content 99.69%; ash content 0.15%; moisture content 0.03%) were obtained from Glanbia plc.

No animals were used in this study, and ethical approval for the use of animals was thus deemed unnecessary.

Model Agglomerated Powder Preparation

The WPI was dispersed at around 60°C for 15 min in deionized water (30%, wt/wt) with a high-shear disperser (Bart Whelan Elec Ltd.) and was then reconstituted for 2 h in a 200-L stainless steel mixing tank with an agitator (BS550, Teagasc Food Research Centre) with agitation (1,200 rpm) followed by overnight storage at 4°C with gentle agitation (500 rpm). Lactose solution (30%, wt/wt) was prepared in deionized water at 70°C for 2 h. Then, WPI-lactose mixtures (30%, wt/wt) with different WPI:lactose ratios (100:0, 75:25, 50:50, and 25:75) were produced and labeled as **WL10**, **WL31**, **WL11**, and **WL13**, respectively. The mixtures (50 kg, determined based on the minimum capability of the spray dryer) were warmed to 80°C and subsequently spray-dried using a pilot-scale 3-stage spray dryer (Anhydro Micraspray 750, Teagasc Food Research Centre) that contains an integrated fluid bed in the main drying chamber and an external fluid bed. The spray dryer also includes a fines return system to inject fines into the product stream at the atomizer (a 2-fluid nozzle atomization system) to agglomerate particles. The feeding rate of the mixture was controlled by a pump and automatically adjusted according to the outlet temperature. Inlet and outlet temperatures of the spray dryer were set at 180°C and 80°C, respec-

tively. The temperature of the powder at the bottom of the drying chamber was around 51°C and that in the agglomeration unit was around 42°C. For each sample, the first 3 to 4 kg of powder was discarded to ensure the spray-drying conditions were stable, and the following powder (8–10 kg) was sampled at different times. There was no significant difference in particle size of samples at different time points; thus, all batches were manufactured at once. All chemical analyses of powders were completed immediately after spray drying; other analyses were performed within 2 mo.

Powder Characterization

Bulk Composition of WPI-Lactose Powders. The lactose content of samples was determined using HPLC with an Aminex HPX 87C fixed ion resin column. Samples were diluted in water and then analyzed to quantify lactose. The eluent was run at 0.5 mL/min and lactose was detected using a refractive index detector with a sensitivity set at 512 mg/L, internal temperature set at 35°C, and positive polarity. Total protein content was measured using the Kjeldahl method to measure total N and calculated using a nitrogen-to-protein conversion factor of 6.38. Total fat contents and the surface-free fat contents of samples were determined as per GEA Niro (2006). The moisture content of powders was determined using the HR83 Hologen Moisture Analyzer (Mettler Toledo International Inc.). The water activity ($\mathbf{a_W}$) of samples was measured using a water activity meter (Novasina LabMaster AW, Novatron Scientific Ltd.).

Surface Composition of WPI-Lactose Powders. The relative surface contents of protein, fat, and lactose (other components such as minerals were ignored) of model samples were calculated from the C, O, and N percentages with a formula of elemental composition of pure milk components (in relative atomic %; for lactose: C, 61.6%, O, 38.4%; milk fat: C, 88.4%, O, 11.6%; whey proteins: C, 68.0%, O, 17.6%, N, 13.8%; Kim et al., 2009; Gaiani et al., 2010). The relative amounts of C, O, and N at the surface of model powder particles were determined by X-ray photoelectron spectroscopy measurements using a Kratos AXIS Ultra spectrometer (Kratos Analytical Ltd.).

Particle Size and Specific Surface Area. The Sauter mean particle size ($\mathbf{D_{3,2}}$) and specific surface area (**SSA**) of model dairy powder samples were measured using a Malvern Mastersizer 3000 (Malvern Instruments Ltd.) with a standard stainless steel venturi feeder. Samples were added to the disperser, and compressed air at 0 bar was used to transport powders. The background measurement time was 20 s, and the sample measurement time was 10 s. Material refractive index and absorption index were 1.45 and 0.1, respectively. The laser obscuration level was at 0.5 to 5%.

Particle Density, Bulk Densities, and Porosity. Bulk density [tapped (100 taps) bulk density (ρ_{tapped}) and loose bulk density (ρ_b)] and particle density (ρ_p) of samples were measured according to GEA Niro (2006) using a jolting volumeter (Funke Gerber) and gas pycnometer (Accupyc II 1340 Gas Pycnometer, Micromeritics Instrument Corp.), respectively. The interparticle porosity (ε) was calculated from Eq. [1]:

$$\varepsilon = 1 - \frac{\rho_{tapped}}{\rho_p}. \quad [1]$$

Powder Structural Properties. A Malvern Morphologi G3 microscope (Malvern Instruments Ltd.) was used to determine the morphology of model powders. Powders were dispersed into a single uniform layer, after which the microscope gradually scanned all the particles and gave the average values of 3 shape factors (circularity, convexity, and elongation; values in the range 0–1). These shape factors are used to quantify how close the shape of a particle is to a perfect circle (Ji et al., 2015). A perfect circle has a circularity of 1 and a smooth shape has a convexity of 1, whereas an irregular or very spiky object has a convexity closer to 0. Elongation is calculated as [1 − aspect ratio]; therefore, a shape symmetrical in all axes, such as a square or circle, has an elongation value of 0.

A scanning electron microscope (Zeiss-Supra 40 VP/Gemini Column) and a polarized light microscope (Instruction BX51, Olympus Optical Co. Ltd.) with a ProgRes camera system (Jenoptik I Optical Systems) were used to observe the structure and morphology of particles from model powders. Samples were mounted on carbon adhesive disks attached to scanning electron microscopy specimen stubs and coated with gold ions in a sputter coater (K575X Sputter Coater, Quorum Technologies) followed by the observation at 2.00 kV. Powders were spread on slides and sunflower oil was used to blend the samples. Coverslips were placed on samples, which were observed with a 60× oil objective or a 10× objective by the polarized light microscope.

Breakage Behavior of Model Samples

Dynamic Breakage Under Different Mechanical Stresses. Model samples with 3 different a_W (~0.01, 0.2, and 0.4) were prepared. The a_W of the initial powders was around 0.2, so the other 2 samples were prepared based on the initial powders. Samples were dried in a vacuum oven at 45°C for 48 h and then transferred immediately to desiccators over P_2O_5 until

the a_W of powder decreased to ~0.01. For samples with a_W of ~0.4, initial samples were kept in desiccators with saturated K_2CO_3 solutions, which gave a relative water vapor pressure (**RVP**) of 44.1% until the a_W of powders reached 0.4. The water content and a_W of samples were determined after sample preparation following the methods described in the section "Bulk Composition of WPI-Lactose Powders."

The dynamic breakage of samples under different mechanical stresses was investigated using the Malvern Mastersizer 3000 because particles could be broken by the 3 mechanisms (velocity gradients caused by impacts between particles, shear stress, and particle-to-wall impacts) during transportation in the powder venturi feeder before measurement of particle size (Bonakdar et al., 2021). There are many similarities between transportation in pneumatic conveyors and venturi feeders (Hazlett et al., 2020; Han et al., 2021a). Thus, transportation in the powder venturi feeder was used to mimic pneumatic conveying conditions at the industrial scale. A low laser obscuration level (0.5–5%) can be used to ensure that most particles undergo similar conditions to dilute-phase pneumatic conveying with breakage occurring at the individual level. In addition, a broad range of air pressures can be controlled in the feeder to provide different mechanical loads so it allows for more conditions than the pneumatic conveyor. Increasing air pressure simulates the increasing air velocity during transportation.

Samples were added to the venturi feeder of the Mastersizer 3000, and the $D_{3,2}$ of samples was measured over a range of air pressures (0, 20, 40, 60, 80, 100, 120, 140, 160, 180, 200, 250, 300, 305, 350, and 400 kPa) following the methods described in "Surface Composition of WPI-Lactose Powders." The degree of powder breakage was shown as the breakage percentage (**BP**), which was the difference of $D_{3,2}$ compared with the initial sample. The BP of samples under certain air pressures was measured according to Eq. [2]:

$$BP = \frac{D_{3,2_0} - D_{3,2_b}}{D_{3,2_0}} \times 100\%, \qquad [2]$$

where $D_{3,2_0}$ and $D_{3,2_b}$ are the $D_{3,2}$ values of powders measured at atmospheric pressure (0 bar) and b bar, respectively.

Breakage During Repeated Laboratory-Scale Dilute-Phase Pneumatic Conveying. Particle breakage occurs when the mechanical load exceeds the intrinsic strength of the particle. Breakage can also happen when mechanical loads lower than the strength of particles are applied multiple times, which is defined as fatigue (Kalman, 1999, 2000; Goder et al., 2002). The susceptibility of model samples to fatigue was investigated by repeated dilute-phase pneumatic conveying tests using a laboratory-scale pneumatic conveyor (as shown in Han et al., 2020). Samples (100 g) were added to the laboratory-scale pneumatic conveying rig with a feeding rate of 3.0 g/s and an air velocity of 40 m/s. Seven samples of each model powder were subjected to the pneumatic conveying test from 1 to 7 times, termed PC1 to PC7, respectively. The particle size of samples was measured after the pneumatic conveying tests following the method described in "Surface Composition of WPI-Lactose Powders."

Influence of Breakage on Functionalities of Model Samples. The PC4 samples from "Breakage During Repeated Lab-Scale Dilute-Phase Pneumatic Conveying" and the initial model powders were used to study the effect of breakage on the functionalities of model powders. The middle sample, PC4, was chosen to avoid the relative extreme treatments—too light or too high.

Rehydration Properties: Wettability and Dispersibility. The wettability of powders was quantified by measuring the wetting time of samples. Wetting time is the time needed to achieve complete wetting of a given quantity of powder without any agitation, and it was measured using a method described by Ji et al. (2016). Distilled water (300 g at 40°C) was added to an 800-mL beaker and powders (4 g) were gently dropped on the surface of the water. The wetting time was the time it took for the immersion of powders in the water.

The dispersibility of samples, represented by the dispersibility index (**DI**), is the proportion of DM that passes through a sieve after mixing the sample with water for a short time. Samples (25 g) were added to a 600-mL beaker with deionized water (100 g at 40°C) and then vigorously mixed with a spatula for 20 s, according to the method described in GEA Niro (2006). The reconstituted samples were poured onto a 180-μm sieve, and samples that passed through were collected for DM content measurement; DI was calculated according to Eq. [3]:

$$DI = \frac{W_1 \times T}{100 - (W_m + T)} \times \frac{100}{w}, \qquad [3]$$

where w is the weight of the sample, W_1 (g) is the weight of water, T (%, wt/wt) is the DM content, and W_m (%, wt/wt) is the free moisture content of the powder.

Water Adsorption, Glass Transition, and Lactose Crystallization Properties. The water adsorption property and time-dependent lactose crystallization of initial and broken model samples at different RVP were measured using the static gravimetric

Table 1. Bulk and surface compositions of initial whey protein isolate (WPI)-lactose model powders[1]

	Bulk sample composition					Surface composition of particles		
Sample[2]	Moisture (%)	Total fat (%)	Total protein (%)	Lactose (%)	Surface free fat (%)	Fat (%)	Whey protein (%)	Lactose (%)
WL10	$5.98^{a} \pm 0.03$	$0.98^{a} \pm 0.01$	$86.47^{a} \pm 0.11$	$1.91^{d} \pm 0.01$	$0.07^{a} \pm 0.01$	$23.6^{ab} \pm 0.6$	$75.6^{a} \pm 0.8$	0.0^{d}
WL31	$4.09^{b} \pm 0.04$	$0.89^{b} \pm 0.01$	$68.94^{b} \pm 0.02$	$22.56^{c} \pm 0.04$	$0.04^{b} \pm 0.01$	$24.5^{a} \pm 4.0$	$66.1^{b} \pm 2.3$	$8.8^{c} \pm 1.8$
WL11	$3.58^{c} \pm 0.02$	0.76^{c}	$45.38^{c} \pm 0.15$	$48.50^{b} \pm 0.01$	$0.03^{b} \pm 0.01$	$7.1^{bc} \pm 0.6$	$63.2^{b} \pm 0.2$	$29.2^{b} \pm 0.8$
WL13	$4.29^{b} \pm 0.01$	$0.65^{d} \pm 0.01$	$23.48^{d} \pm 0.02$	$71.66^{a} \pm 0.05$	0.00^{c}	$0.5^{c} \pm 0.3$	$50.3^{c} \pm 1.5$	$48.5^{a} \pm 1.4$

[a–d]Means different values within columns are significantly different at $P < 0.05$.

[1]Values are mean ± SE ($n \geq 2$).

[2]WL10, WL31, WL11, and WL13 had WPI:lactose ratios of 100:0, 75:25, 50:50, and 25:75, respectively.

method. Samples (1 g) were dried in a vacuum oven at 45°C for 48 h and equilibrated at 25°C for 168 h at different RVP provided by different saturated salt solutions: NaCl, $NaNO_2$, $Mg(NO_3)_2$, K_2CO_3, $MgCl_2$, CH_3COOK, and LiCl, which gave RVP of 76.1, 65.6, 54.5, 44.1, 33.2, 23.1, and 11.4%, respectively. Samples were weighed at 0, 3, 6, 9, 12, and 24 h and then at 24-h intervals until 312 h. Results are presented as the equilibrated water content in 100 g of DM.

The glass transition temperature ($\boldsymbol{T_g}$, inflection point) and initial crystallized temperature ($\boldsymbol{T_{ic}}$, peak) of samples (equilibrated at different RVP: 11.4, 23.1, 33.2, and 44.1%) were determined using a differential scanning calorimeter (DSC Q2000, TA Instruments), following the method described by Li et al. (2016b).

Statistical Analysis

The experimental design was completely randomized. Measurements of moisture content, particle size, SSA, dynamic breakage under different mechanical stresses, rehydration, and water adsorption properties were performed in triplicate; all other measurements were carried out in duplicate. Student's *t*-test with a 95% confidence interval was used to determine significant differences between samples before and after breakage in each model powder. One-way ANOVA with Tukey's test (IBM SPSS Statistics version 24; IBM Corp.) was used to determine significant differences between each initial model sample with a significance level of $P < 0.05$.

RESULTS AND DISCUSSION

Powder Bulk and Surface Composition

The bulk and surface composition of 4 initial model samples are presented in Table 1. Whey protein content ranged from 86.5 to 23.5%, and lactose contents ranged from 1.9 to 71.7% for agglomerated WPI-lactose powders. The moisture contents of samples were different; sample WL10 had the highest moisture content ($P < 0.05$). The total fat contents and surface-free fat contents of all samples decreased with decreasing whey protein content because the fat in the model samples came from WPI instead of lactose.

From the X-ray photoelectron spectroscopy results, lactose content on the surface of particles increased and whey protein and fat contents decreased with decreasing bulk protein content of model samples, consistent with the changing trend of their bulk composition. However, the composition on the surfaces of model sample particles was very different from their bulk composition. The fat contents on the surface of particles from WL10 and WL31 were around 24%, which is much higher than their bulk fat contents. Also, the highest content on the surface of particles was whey protein, ranging from 50% to 76%, even for WL11 and WL13, whose bulk lactose contents were greater than 50%. Unlike fat and protein, the lactose concentration on the particle surfaces was lower than that of the bulk composition. Similar results have been found in some commercial milk particles, such as low-fat model powder, skim milk powder (**SMP**), whole milk powder, SMP-lactose mixtures, milk protein concentrate, and demineralized whey powder (Shrestha et al., 2007; Kim et al., 2009; Foerster et al., 2016). These results might be because of the different migration properties of milk components toward the interior or surface of the droplet during the atomization stage and the subsequent drying stage, resulting in redistribution of the components within the particles (Shrestha et al., 2007). Based on the Stoke-Einstein equation, the descending size order of powder components is free fat particles or fat globules > casein micelles > whey protein > lactose > salts, whereas their diffusivities follow the inverse order (Kim et al., 2003). Therefore, during drying after atomization, lactose very quickly diffuses toward the center of the droplet, followed by whey protein and free fat or fat globules. However, some researchers have demonstrated that fat globules rupture and spread homogeneously over the droplet surface, creating a thin

fat film during the atomization stage and resulting in a higher surface fat content than bulk fat content (Foerster et al., 2016). The difference in surface composition of model samples may affect breakage by altering the cohesiveness of powders; fat on the surface increases the cohesiveness of bulk samples. Also, uneven distribution of ingredients throughout the particles may lead to differences in powder functionalities and properties before and after breakage.

Powder Physical Properties

Some physical properties of the 4 initial model samples are shown in Table 2. The physical properties of spray-dried powders are determined by powder composition, processing conditions (e.g., preheat treatment, homogenization, and concentration), spray-drying parameters (e.g., atomization parameters and drying temperature), and other treatments on milk concentrates or on final powder products (e.g., sonication treatment and ozone treatment; Chandrapala et al., 2012; Balde and Aïder, 2017; Er et al., 2019; Sert and Mercan, 2021; Sert et al., 2021). In this study, the physical properties of WPI-lactose powders differed with differences in ingredients. The $D_{3,2}$ of WL13 and WL11 were significantly higher ($P < 0.05$) than those of WL31 and WL10, which differs from nonagglomerated milk protein isolate-lactose model powders, in which a higher protein content results in larger particles (Li et al., 2016a,c). This might be because the higher lactose content made the mixture liquid stickier, and lactose worked as the binder during agglomeration, increasing the efficiency of agglomeration and producing larger particles. It should be noted that β-LG exists naturally as a dimer, which unfolds at temperatures above 65°C, exposing a free sulfhydryl group that is normally buried. This activated form of β-LG can then react with other molecules of β-LG and other whey proteins such as α-LA or BSA via disulfide linkages. The heat-induced denaturation of β-LG and the subsequent protein–protein interactions would form whey protein aggregates and increase the particle size of the mixture, which may influence the size of the final particles.

Previous research has shown that particle size is an important factor affecting dairy powder breakage; under the same processing conditions, the degree of breakage increases as the particle size increases when the particle structure was similar (Han et al., 2021a). This is due to the possibility of more imperfections in larger particles, such as internal holes and cracks where the highest local tensile stress will be generated, leading to initiation and propagation of fractures (Antonyuk et al., 2005). In addition to having fewer flaws, small particles are harder to break because the interparticle forces (such as

Table 2. Physical and morphological properties of initial whey protein isolate (WPI)-lactose model powders[1]

Sample[2]	Particle size [$D_{3,2}$ (μm)]	SSA[3] (m^2/kg)	Particle density (kg/L)	Loose bulk density (kg/L)	Tapped bulk density (kg/L)	Porosity (%)	Morphological characteristic		
							Elongation	Circularity	Convexity
WL10	$47.5^{c} \pm 0.1$	$120.4^{b} \pm 0.2$	$1.008^{a} \pm 0.001$	$0.217^{b} \pm 0.003$	$0.329^{a} \pm 0.001$	$67.32^{a} \pm 0.01$	$0.199^{d} \pm 0.003$	$0.861^{a} \pm 0.019$	$0.987^{a} \pm 0.002$
WL31	$43.5^{d} \pm 0.1$	$131.6^{a} \pm 0.3$	$0.938^{b} \pm 0.001$	$0.217^{b} \pm 0.002$	$0.316^{a} \pm 0.005$	$66.27^{b} \pm 0.17$	$0.205^{c} \pm 0.001$	$0.851^{b} \pm 0.001$	$0.986^{b} \pm 0.003$
WL11	$72.8^{b} \pm 0.1$	$78.5^{c} \pm 0.1$	$0.850^{c} \pm 0.001$	$0.228^{b} \pm 0.001$	$0.316^{a} \pm 0.001$	$62.80^{c} \pm 0.04$	$0.243^{b} \pm 0.001$	$0.822^{c} \pm 0.001$	$0.983^{c} \pm 0.003$
WL13	$86.6^{a} \pm 0.1$	$66.0^{d} \pm 0.1$	$0.851^{c} \pm 0.001$	$0.247^{a} \pm 0.002$	$0.331^{a} \pm 0.002$	$61.15^{d} \pm 0.02$	$0.249^{a} \pm 0.002$	$0.805^{d} \pm 0.002$	$0.977^{d} \pm 0.003$

[a–d]Means different values within columns are significantly different at $P < 0.05$.

[1]Values are mean ± SE (n = 2 for morphological properties and n = 3 for the other properties).

[2]WL10, WL31, WL11, and WL13 had WPI:lactose ratios of 100:0, 75:25, 50:50, and 25:75, respectively.

[3]Specific surface area.

liquid bonds, electrostatics, and van der Waals forces) that bind particles together are stronger (Reynolds et al., 2005). This may result in higher degrees of breakage for WL13 and WL11 than for WL31 and WL10 under the same mechanical stress. As WL31 and WL10 had smaller particle sizes, they also had larger SSA values.

The particle densities of WL31 and WL11 were similar, at around 0.85 kg/L, significantly lower than those of high-protein model powders, at around 1.0 kg/L ($P < 0.05$). The particle densities of these model powders were much lower than those of nonagglomerated WPI-lactose model powders, at around 1.3 kg/L. Particle density is the mass per unit volume of particles, which includes closed internal holes but not cracks or open holes, so it is associated with particle structure characteristics that also affect the dynamic breakage of dairy powder particles. Rather than affecting individual particles, porosity affects the properties of bulk particles. The porosity of our model powders decreased with increasing lactose content ($P < 0.05$); the porosities of WL13 and WL11 were similar, and those of WL13 and WL10 were similar. Compared with their loose bulk densities, tapped bulk densities were more similar, at around 0.32 kg/L. The loose bulk densities of WL10 and WL 31 were lower, which might be because the particle sizes were small; these small particles were lighter and had higher SAA and thus trapped air more easily in a bed of powder. Also, their flowability was very poor, which resulted in large packing irregularities during sample filling.

Powder Morphology and Structure

Three morphological characteristics (circularity, convexity, and elongation; Table 2) and scanning electron and light microscopy photographs (Figure 1) of particles from initial model powders were used to identify particle shapes and microstructures of samples. Previous research shows that the extent and type of breakage are heavily dependent on the structure and shape of agglomerates (Golchert et al., 2004; Norazirah et al., 2016); the more spherical a particle is, the greater its strength (Deng and Davé, 2017). The discrete element model simulation results showed differences in nonspherical and spherical agglomerate breakage because the degree of breakage in nonspherical agglomerates depends not only on the interface energy, impact angle, and impact speed but also on orientation (Liu et al., 2010). Considering particle structure, the strength of crystals and continuum solids was higher than particles with internal holes, because the internal holes were the defective zones (Han et al., 2021c). The number, distribution, and size of internal holes also affect the strength of particles. Particle shape and structure are affected by the parameters of the powder drying process and powder composition.

As can be seen in Figure 1, the particles from model powders were clearly agglomerated and there was no crystallized lactose. As seen in the scanning electron micrographs, the shape and structure of the primary particles from the 4 samples were similar, likely because the atomization stage and spray-drying parameters were the same. Most of the primary particles were hollow sphere particles with numerous holes of different sizes throughout the particles. Compared with WL13 primary particles, which had a "shriveled" surface, the surface of primary particles from the other 3 samples (that contained less lactose) was smoother. This has been reported in previous studies on milk protein powders, SMP, and model IMF (Kim et al., 2009; Murrieta-Pazos et al., 2011; McCarthy et al., 2013; Maidannyk et al., 2020). The light microscopy photographs showed that WL13 and WL11 were more agglomerated than WL31 and WL10, which resulted in differences in their particle size. After agglomeration, particles were irregular, and the irregularity of particles increased with increasing lactose content ($P < 0.05$), as shown by the decreases in circularity and convexity, and the increase in elongation, especially for WL11 and WL13 (Table 2). Thus, higher particle size and more irregular particle shapes might result in lesser particle strength and greater particle breakage for model samples that contain more lactose. Also, some of the primary particles on the surface of agglomerates were broken and the internal holes were exposed, especially for WL13, in which the particle surface was very rough. This is because agglomeration and breakage of particles occur concurrently during granulation (Reynolds et al., 2005). Breakage affects the strength and homogeneity of agglomerates and is an important rate process during agglomeration. Also, the connection areas between primary particles in WL13 were larger than those of the other 3 samples, which might make the structural strength of particles in WL13 greater than that of other samples.

Dynamic Breakage Under Different Mechanical Stresses

The dynamic breakage of initial agglomerated WPI-lactose model powders (with a_W 0.2) under different mechanical stresses in the venturi feeder was represented by a series of BP (Figure 2). For each sample, BP increased with increasing air pressure. This is because increasing the air pressure increases the air velocity, which in turn increases the particle speed. Hence, higher

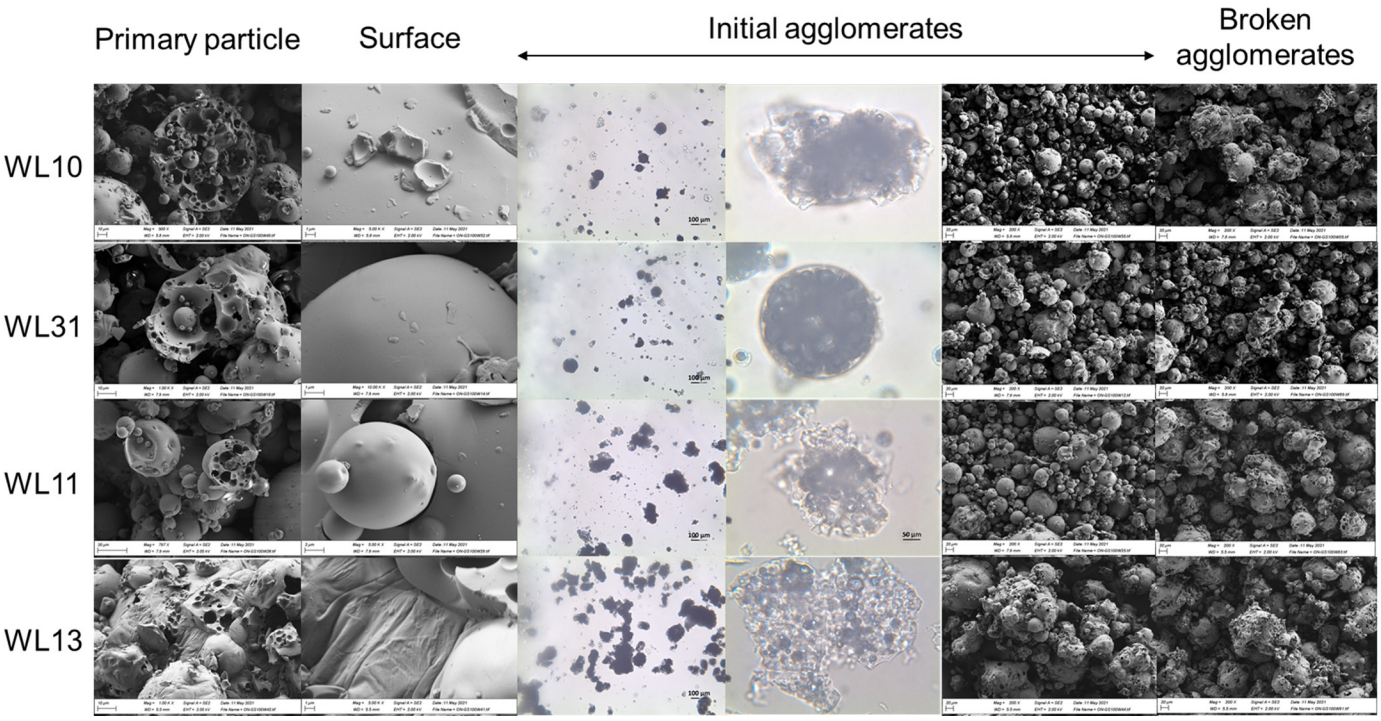

Figure 1. Micrographs of initial and broken whey protein isolate (WPI)-lactose model particles. WL10, WL31, WL11, and WL13 had WPI: lactose ratios of 100:0, 75:25, 50:50, and 25:75, respectively. Broken agglomerates were sampled after 4 times of transportation by laboratory-scale dilute-phase pneumatic conveying at 40 m/s.

air pressure means more severe particle collisions, which causes more breakage. The BP of each model powder increased logarithmically with increasing air pressure, which is consistent with previous studies on the breakage of some agglomerated or nonagglomerated dairy powders, such as SMP, IMF, and WPI, among others. From Figure 2, no significant difference can be seen in BP between initial WL31 and WL10 powders, because their particle size and structure were similar. The BP of WL13 and WL11 was higher than that of the other 2 samples, which could be explained by their larger particle size ($P < 0.05$, when air pressure $\geq$20 kPa), greater elongation, and lower convexity and circularity. For the same reason, the BP of WL13 was higher than that of WL11 ($P < 0.05$, when air pressure $\geq$20 kPa). These results indicate that, for WPI-lactose agglomerates, the degree of breakage increased with increasing lactose content of powders under the same processing conditions because of the increase in the particle size and the more irregular particle shapes; however, the breakage of WPI and agglomerates containing 25% lactose was similar. This was not observed in nonagglomerated WPI-lactose powders (whey protein content ranged from 80 to 20%, and lactose contents were from 20 to 80%) and their BP were similar, which could be because of their comparable particle sizes (from 6.1 to 7 μm).

The BP of 4 powders with 3 different a_W at different air pressures are given in Figure 3. For each sample, the BP of dried powders (at a_W 0.02) was similar to that of their initial powders (a_W 0.2) but the BP of high-water-

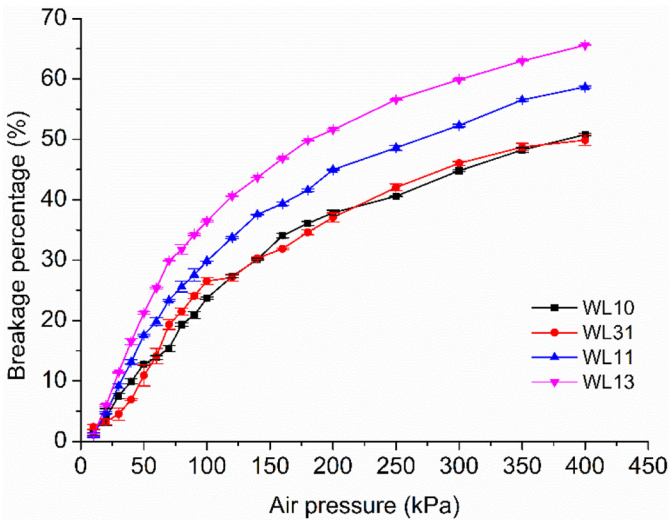

Figure 2. Breakage percentages of initial whey protein isolate (WPI)-lactose model powders (with water activity of 0.2) during transportation by the powder venturi feeder at different air pressures. WL10, WL31, WL11, and WL13 had WPI:lactose ratios of 100:0, 75:25, 50:50, and 25:75, respectively. Error bars represent SD.

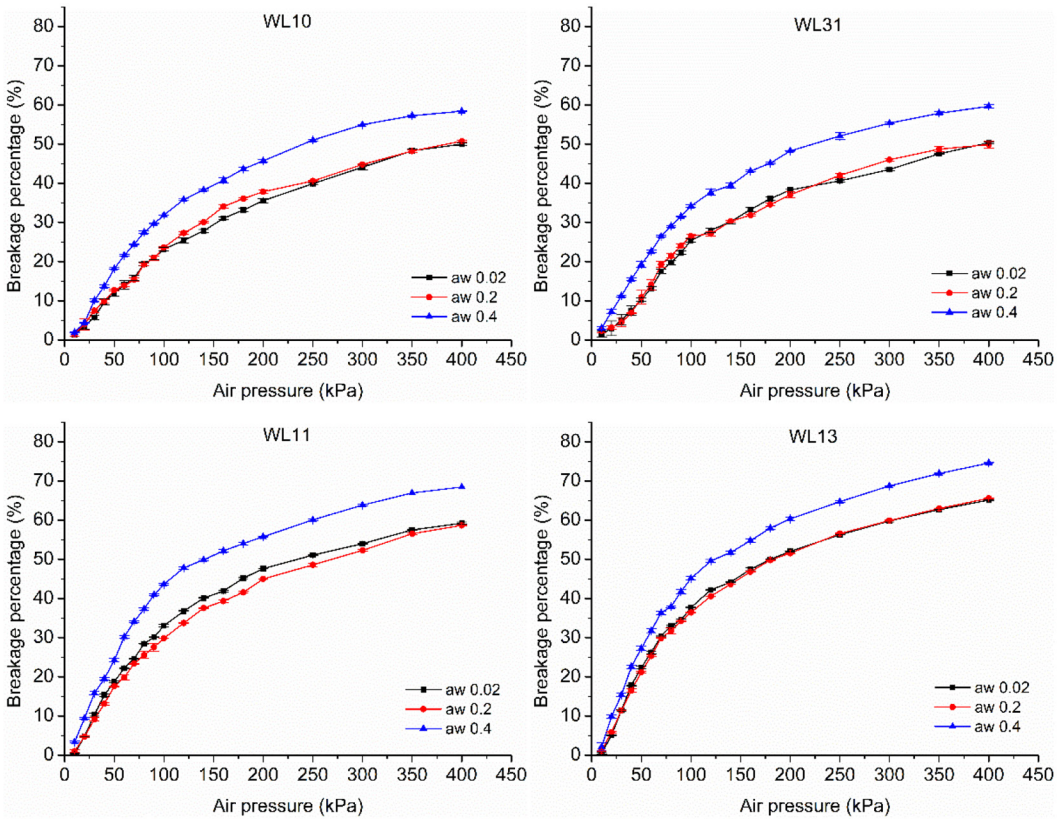

Figure 3. Breakage percentages of whey protein isolate (WPI)-lactose model powders with different water activities (a_w; 0.02, 0.2, and 0.4) during transportation by the powder venturi feeder at different air pressures. WL10, WL31, WL11, and WL13 had WPI:lactose ratios of 100:0, 75:25, 50:50, and 25:75, respectively. Error bars represent SD.

content powders (a_W 0.4) was much higher than that of the initial powders. Previous studies have reported that during the vibration test of agglomerated skim milk powder, greater breakage occurred in samples with a higher a_W (0.44) than in those with a lower a_W (0.2; Yan and Barbosa-Cánovas, 2001a). These results indicate that removing the initial moisture did not affect the breakage of model powders, but increasing the moisture content within a certain range at the base of initial powders could reduce powder strength. This might be because the drying process only removed the moisture inside particles but did not change the particle structure and texture; the particle sizes between samples at a_W 0.02 and 0.2 were not significantly different ($P > 0.05$, data not shown). In contrast, the particle size of samples at a_W 0.4 was greater than that of their initial samples; for example, the particle size of WL13 increased from 86.6 to 93.0 μm when its a_W increased from 0.2 to 0.4. Increased water content can also soften the material of powders, particularly the water-soluble components, which would deform powders and decrease their strength (Rennie et al., 1999; Kim et al., 2005). In addition, the main agglomeration mechanism for materials in the agglomerated state is the formation of powder bridges using binders (e.g., lactose). Humidifying the agglomerates can change particle surfaces by local plasticization, liquid layer formation, or solubilization, which may decrease the strength of bridges or affect the other properties of binders (Samimi et al., 2003).

Breakage Under Repeated Mechanical Stresses: Effect of Fatigue

Particles can break in a single collision during pneumatic conveying when the impact load is greater than its strength. Additionally, repeated lower-impact loads can cause breakage, which is known as fatigue. Under these circumstances, although the first impact may not break particles, it might lead to cracks, which makes particles more sensitive to the next impact. In factories, there are many bends in the pneumatic conveying system and powders are repeatedly transported during processes such as receiving, packing, reprocessing, and storage (Konami et al., 2002). Therefore, the

breakage caused by repetitive transport should be considered.

The effect of fatigue on WPI-lactose agglomerates was shown as the change in particle size after each instance of laboratory-scale dilute-phase pneumatic conveying with an air velocity of 40 m/s, as shown in Figure 4A. For all samples, the changes in particle size after different instances (from 1 to 7) of pneumatic conveying were different. Based on previous research, under the same processing conditions, the degree of breakage decreases with decreasing particle size. When increasing the number of pneumatic conveying tests, the particle size of samples gradually decreased and the degree of breakage did decrease, but not gradually, which means cracks were produced and decreased the strength of particles, which led to a high degree of breakage for some smaller particles. These results imply that fatigue affected the breakage of WPI-lactose agglomerates, especially for high-lactose powders, which might be because of their larger particle size and more irregular particle shapes. These findings also mean that increasing the particle size or particle irregularity might increase the effect of fatigue on the degree of breakage, which is consistent with results obtained from research on the breakage of detergent agglomerates (Samimi et al., 2003). The cumulative breakage of WL13 and WL11 was much greater ($P < 0.05$) than that of the other samples (Figure 4B), which was consistent with the results of BP under different mechanical stresses (Figure 2) and confirmed that breakage was greater for the higher lactose powders.

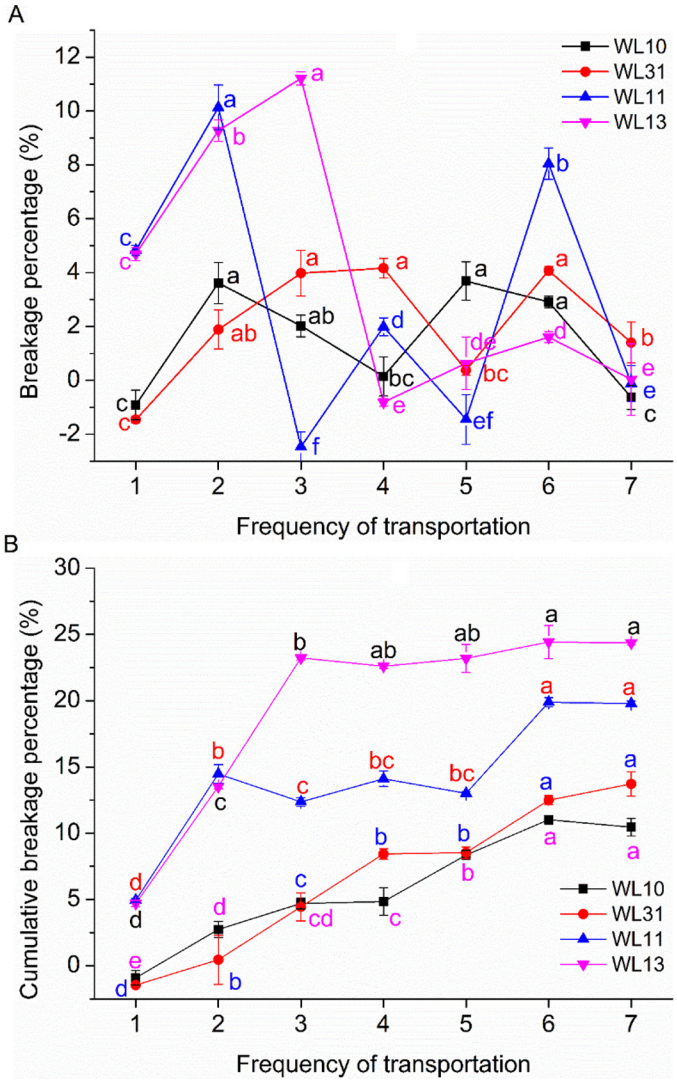

Figure 4. Breakage percentages of whey protein isolate (WPI):lactose model powders after each time of transportation by laboratory-scale dilute-phase pneumatic conveying at 40 m/s compared with previously transported powders (A) or initial powders (B). WL10, WL31, WL11, and WL13 had WPI:lactose ratios of 100:0, 75:25, 50:50, and 25:75, respectively. Error bars represent SD.

Rehydration Properties of Model Samples After Breakage

The effect of breakage on the wettability and dispersibility of WPI-lactose model agglomerates was investigated by comparing properties of initial samples and broken samples produced by 4 times (PC4) of dilute-phase pneumatic conveying. The scanning electron micrographs and some properties of broken powders are shown in Figure 1 and Supplemental Table S1 (https://doi.org/10.5281/zenodo.5573837; Han et al., 2021d), respectively, and the changes in physical and structural properties before and after breakage may affect functionalities of model powders. From the scanning electron micrographs, we can see that breakage changed the morphology of particles: primary particles on agglomerate surfaces were broken and particle surfaces became very rough, especially for WL13 and WL11. These changes decreased the particle size [$D_{3,2}$ decreased 4.8% ($P = 0.023$), 4.6% ($P = 0.01$), 12.4% ($P = 0.01$), and 23.8% ($P = 0.000$) for WL10, WL31, WL11, and WL13, respectively] and increased the SSA [SSA increased 5.1% ($P = 0.027$), 9.1% ($P = 0.000$), 16.4% ($P = 0.01$), and 31.2% ($P = 0.000$) for WL10, WL31, WL11, and WL13, respectively] and particle density [particle density increased 19.5% ($P = 0.002$), 20.0% ($P = 0.001$), 22.0% ($P = 0.001$), and 11.7% ($P = 0.001$) for WL10, WL31, WL11, and WL13, respectively], which is consistent with previous research (Boiarkina et al., 2016; Han et al., 2020; Hazlett et al., 2020; Zhang et al., 2020). Also, the larger the particles, the greater the changes that occurred. Furthermore, the surface composition changed after breakage

because of exposure of the interior of the particles, as seen with the increase in lactose content [lactose content increased 61.4%, 8.9%, and 9.5% for WL31, WL11, and WL13, respectively ($P > 0.05$)] and the slight decrease in whey protein [whey protein content decreased 9.2% and 9.7% for WL11 and WL13, respectively ($P > 0.05$)].

The wetting process is the first step of rehydration and reflects the ability of particles to overcome the surface tension between them and absorb a liquid based on capillary force (Ji et al., 2016). The wetting time of model powders before and after breakage is shown in Figure 5. For this method, powders are considered nonwettable if the wetting time is longer than 2 min (GEA Niro, 2006). As shown in Figure 5, only WL13 was wettable, with a wetting time of 1.6 min. In this study, the wetting time of the other 3 samples was compared to show the effect of breakage on wettability, even though the latter samples were not wettable. As shown in Figure 5, wettability significantly decreased after breakage for WL13 ($P = 0.039$) and WL11 ($P = 0.006$), especially for WL13 where the wetting time increased by 38%. This is not surprising because their particle size decreased, and this is consistent with previous research on IMF, fat-filled milk powder, and whey protein concentrate powders (Han et al., 2020; Hazlett et al., 2020). In contrast, the wetting time of WL31 ($P = 0.033$) and WL10 ($P = 0.031$) was significantly decreased. This might be because these samples contained high protein contents that had poor wettability when particles were small, whereas breakage roughened the surface of particles and exposed more internal holes, which might increase water penetration into the particles. This could also be because of the changes in the particles' surface composition (Supplemental Table S1, https://doi.org/10.5281/zenodo.5573837). Both samples showed a reduction in surface fat content, and W31 showed an increase in surface lactose content, which could reduce wetting time. These results imply that breakage could increase the wetting time of wettable samples but decrease the wetting time of powders with poor wettability.

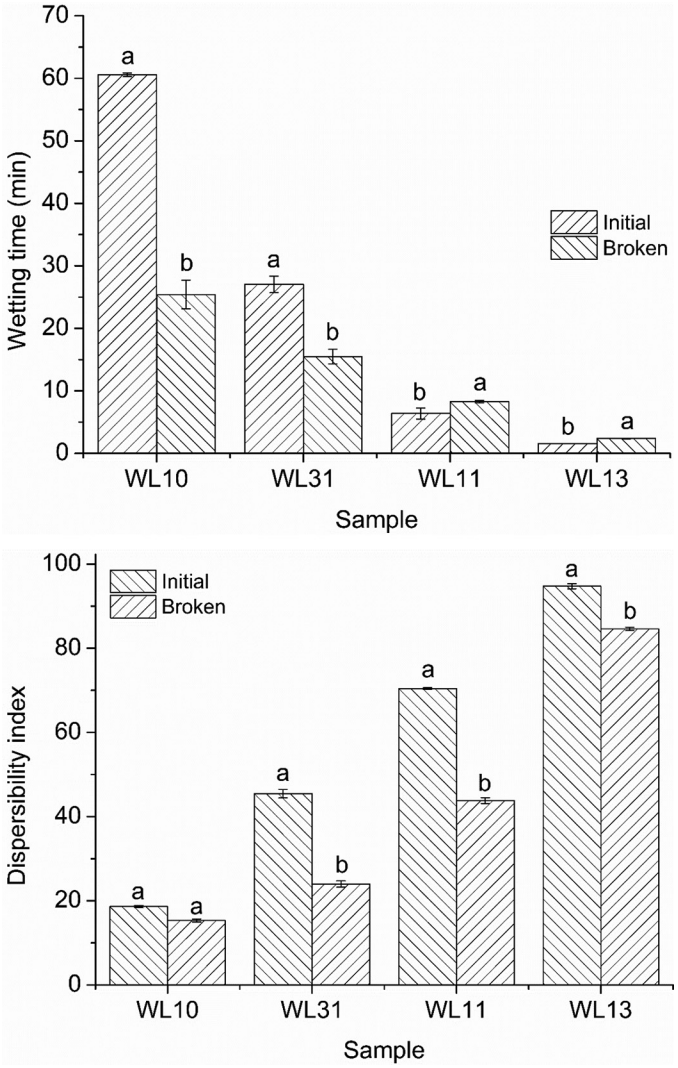

Figure 5. Wetting time and dispersibility index of initial and broken (after 4 times of transportation by laboratory-scale dilute-phase pneumatic conveying at 40 m/s) whey protein isolate (WPI)-lactose model powders. WL10, WL31, WL11, and WL13 had WPI:lactose ratios of 100:0, 75:25, 50:50, and 25:75, respectively. Within a sample, bars with different letters (a, b) are significantly different at $P < 0.05$. Error bars represent SD.

After the wetting process, particles need to be dispersed into water before dissolving (Goalard et al., 2006). Figure 5 shows the effect of breakage on the DI of the 4 WPI-lactose model powders. Dispersibility increased with increasing lactose content because lactose disperses much more easily than whey protein. Breakage reduced the dispersibility of all powder samples because of the decrease in particle size, which makes it harder for water to penetrate into the powder bulk. Similar findings were observed in IMF, fat-filled milk powder, and whey protein concentrate powders (Han et al., 2020; Hazlett et al., 2020). The DI of WL11 and WL31 were more affected than those of the other 2 samples, perhaps because the dispersibility of WL13 and WL10 was more influenced by their composition. For example, the DI of WL13 was the highest because it contained a large amount of hydrophilic lactose, which makes it easy for water to penetrate into the agglomerates and thereby sinking and dispersing quickly. The dispersibility was still good even with a 20% decrease in particle size, whereas the opposite was true for WL10. These results imply that breakage decreased the dispersibility of model samples, especially for samples with moderate dispersibility (DI was around 50%).

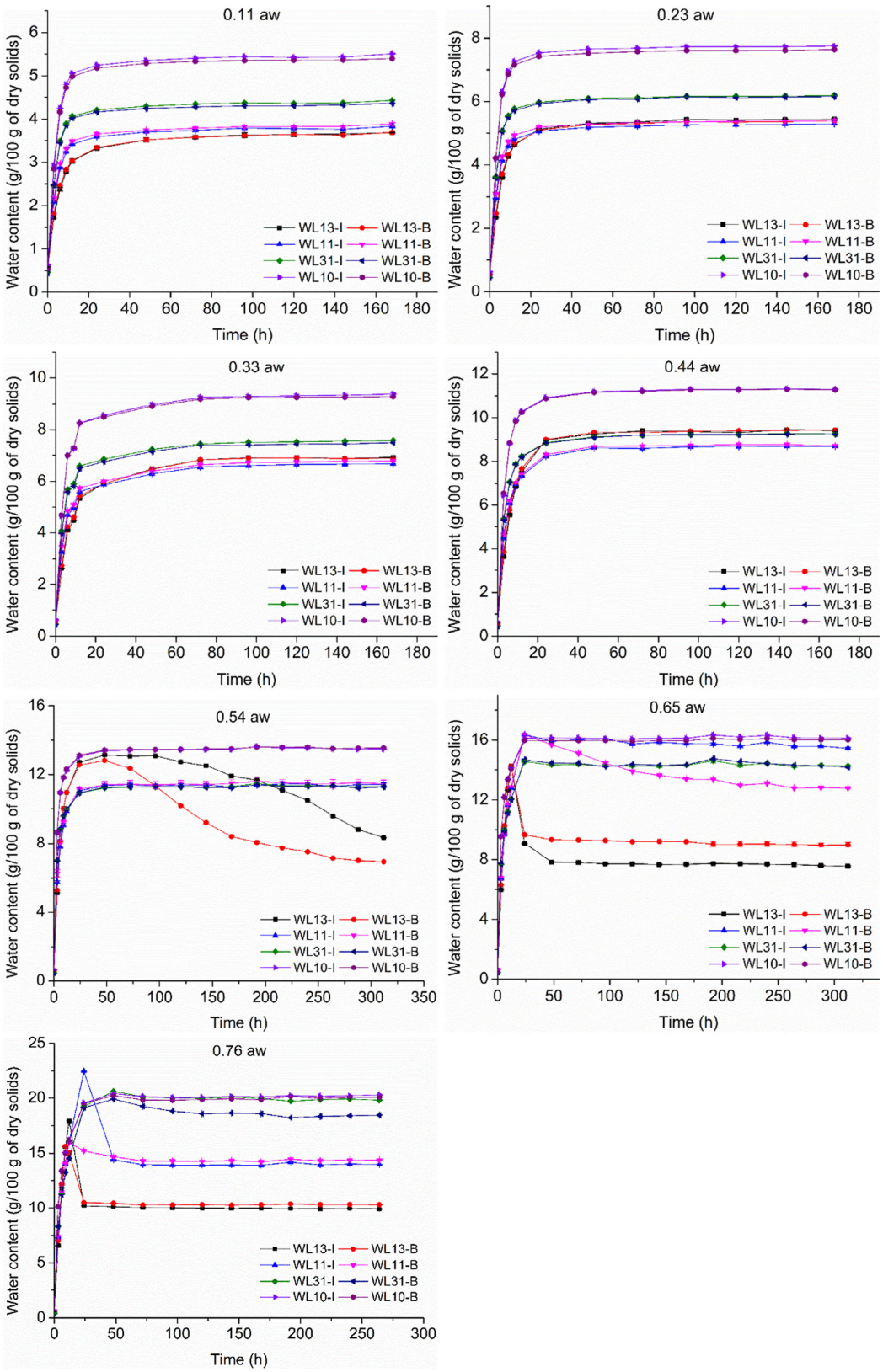

Figure 6. Water sorption behavior of initial (-I) and broken (-B; after 4 times of transportation by laboratory-scale dilute-phase pneumatic conveying at 40 m/s) whey protein isolate (WPI)-lactose model powders equilibrated at various water activities (a_w; 0.11 to 0.76) for 168 or 312 h at 25°C. WL10, WL31, WL11, and WL13 had WPI:lactose ratios of 100:0, 75:25, 50:50, and 25:75, respectively. Error bars represent SD.

Table 3. Glass transition temperature (T_g, inflection point) and initial crystallization temperature (T_{ic}, peak) of whey protein isolate (WPI)-lactose model powders stored for 168 h at various water activities (0 to 0.44) at 25°C[1]

		Water activity				
Sample[2]	Timepoint	0	0.11	0.23	0.33	0.44
WL10						
T_g	Initial	—	—	—	—	—
	PC4[3]	—	—	—	—	—
T_{ic}	Initial	—	145.6 ± 0.9	143.3 ± 0.1	138.9 ± 0.2	142.7 ± 0.4
	PC4	—	147.4 ± 0.3	142.9 ± 0.4	138.9 ± 0.2	141.2 ± 0.4
WL31						
T_g	Initial	—	86.1 ± 0.1	66.8 ± 0.9	55.4 ± 0.7	42.1 ± 0.1
	PC4	—	87.2	67.8 ± 0.2	58.2 ± 0.5	42.4 ± 0.7
T_{ic}	Initial	—	149.1 ± 0.1	147.2 ± 0.2	144.4 ± 0.6	146.0 ± 0.3
	PC4	—	148.5 ± 0.2	146.6 ± 0.1	145.9 ± 0.2	144.5 ± 0.4
WL11						
T_g	Initial	121.8 ± 0.3	74.1 ± 0.2	60.1 ± 0.2	48.5 ± 0.1	32.6 ± 0.1
	PC4	122.0 ± 0.2	73.8 ± 0.1	60.0 ± 0.1	48.3 ± 0.2	33.7 ± 0.2
T_{ic}	Initial	—	152.7 ± 0.2	151.5 ± 0.1	148.2 ± 0.1	148.1 ± 0.3
	PC4	—	152.7 ± 0.1	149.6 ± 0.1	145.3 ± 0.2	137.7 ± 0.2
WL13						
T_g	Initial	115.7 ± 0.3	69.6 ± 0.2	53.8 ± 0.3	42.7 ± 0.4	26.4 ± 0.6
	PC4	115.6 ± 0.1	69.8 ± 0.7	53.4 ± 0.1	42.3 ± 0.1	25.7 ± 0.1
T_{ic}	Initial	—	144.0 ± 0.1	129.1 ± 0.1	117.0 ± 0.1	95.2 ± 0.2
	PC4	—	134.7 ± 0.4	118.6 ± 0.1	105.8 ± 0.1	86.0 ± 0.1

[1]Values are mean ± SE (n = 2).

[2]WL10, WL31, WL11, and WL13 had WPI:lactose ratios of 100:0, 75:25, 50:50, and 25:75, respectively.

[3]PC4 = powders after 4 times of transportation by laboratory-scale dilute-phase pneumatic conveying at 40 m/s.

Water Adsorption, Glass Transition, and Lactose Crystallization

Water adsorption behavior at several a_W (0.11–0.76 a_W) of model powders before and after breakage was plotted as a function of time (Figure 6). The water adsorption behavior at all a_W, and the final water contents of WL10 were not affected by breakage. For the other 3 samples that contained lactose, breakage did not affect water adsorption rate or final water contents at a_W from 0.11 to 0.44 but accelerated their time-dependent crystallization at $a_W \geq 0.54$; the higher the lactose content, the greater the impact. Only WL13 was influenced by breakage on time-dependent crystallization at 0.54 a_W, and the water content decreased earlier and faster for broken samples. Similarly, the time-dependent crystallization of WL11 and WL31 was accelerated by breakage at the initial a_W of 0.66 and 0.76, respectively, which was presumably caused by protein interference with lactose crystallization, which has been previously reported (Shrestha et al., 2007). The final water contents after crystallization of breakage samples were slightly higher than that of initial samples for WL13 and WL11 at $a_W \geq 0.65$. This is different from results of a previous study (Han et al., 2022) on the effect of breakage mechanisms on the water adsorption behavior of IMF, where the final water content of samples after crystallization was not influenced by breakage. This difference might be because of the difference in the composition of the IMF samples and the WPI-lactose agglomerates. In addition, at all a_W, the final water contents of powders increased with increasing protein content. It should be noted that, lactose, a reducing sugar, can interact with amine groups of proteins, particularly the ε-amino group of lysine, in the initial step of the Maillard reaction. This lactose–protein interaction is initiated during heat treatment but continues during storage; in some products, lactosylated proteins constitute a significant proportion of the total proteins. Lactosylation occurs readily in the dry state and produces ε-*N*-deoxylactulosyl-D-lysine or lactulosyl lysine, which results in more lactose units attached to β-LG (Deeth and Hartanto, 2009). Therefore, after storage, lactosylation might influence powder water sorption behavior. The results indicate that breakage did not affect the water adsorption rate or final water content of WPI-lactose agglomerates at low a_W but it did accelerate time-dependent crystallization and slightly increased the final water content after crystallization.

The T_g (inflection point) and T_{ic} (peak) of samples over the a_W range of 0 to 0.44 are shown in Table 3. We found that at the same a_W, T_g increased with decreasing lactose content and increasing protein content, which was because protein absorbed most of the water, leav-

ing less water available for lactose plasticization and subsequent crystallization, as was reported by Shrestha et al. (2007). For the same sample, T_g decreased with increasing a_W because of the higher water content. For each sample at all a_W, no significant differences in T_g were found between the initial and breakage samples because of their similar final water contents. Different from T_g, the initial crystallized temperatures were decreased by breakage, especially for samples that contained high lactose content; the higher the lactose content, the greater the decrease in the initial crystallized temperatures. The T_{ic} of WL13 decreased by around 10°C after breakage at $a_W \leq 0.44$, even thought there was no difference in the final water content of initial and breakage samples. Overall, breakage did not affect the T_g of WPI-lactose agglomerates but decreased the T_{ic} of powders that contained lactose.

CONCLUSIONS

The whey protein and lactose composition of powders affected breakage by influencing the particle size and structure of the agglomerates formed under the same drying conditions. The 2 powders with higher protein content had smaller particle size, were more regular in shape, and had higher particle densities, which resulted in less breakage compared with the 2 higher lactose powders. Removing the initial moisture did not affect the breakage of powders but increasing the moisture content within a certain range increased breakage. Fatigue affected the breakage of WPI-lactose agglomerates, especially for the 2 higher lactose powders. Breakage changed the morphology and surface composition of particles, decreasing particle size and increasing SSA and particle density. These changes decreased the dispersibility of samples, increased the wetting time of wettable samples, but decreased the wetting time of powders with poor wettability. Also, breakage accelerated time-dependent crystallization and decreased the T_{ic} of powders that contained lactose. Overall, our results confirm that under the same drying conditions, powder formulation significantly affected breakage by affecting the physical properties of powder particles. Further research on the effect of other milk powder ingredients in more complex powders on breakage will be useful.

ACKNOWLEDGMENTS

This research was funded by the Teagasc, Agriculture and Food Development Authority of Ireland under project 0153. The authors acknowledge Helen Slattery and Martina O'Brien (Teagasc Food Research Centre, Moorepark, Fermoy, Co. Cork, Ireland) for the measurement of powder composition. The authors have not stated any conflicts of interest.

REFERENCES

Antonyuk, S., J. Tomas, S. Heinrich, and L. Mörl. 2005. Breakage behaviour of spherical granulates by compression. Chem. Eng. Sci. 60:4031–4044. https://doi.org/10.1016/j.ces.2005.02.038.

Balde, A., and M. Aïder. 2017. Effect of cryoconcentration, reverse osmosis and vacuum evaporation as concentration step of skim milk prior to drying on the powder properties. Powder Technol. 319:463–471. https://doi.org/10.1016/j.powtec.2017.07.016.

Boiarkina, I., C. Sang, N. Depree, A. Prince-Pike, W. Yu, D. I. Wilson, and B. R. Young. 2016. The significance of powder breakdown during conveying within industrial milk powder plants. Adv. Powder Technol. 27:2363–2369. https://doi.org/10.1016/j.apt.2016.10.019.

Bonakdar, T., M. Ali, and M. Ghadiri. 2021. Particle breakability assessment using an Aero S disperser. Int. J. Pharm. 597:120365. https://doi.org/10.1016/j.ijpharm.2021.120365.

Chandrapala, J., G. J. O. Martin, B. Zisu, S. E. Kentish, and M. Ashokkumar. 2012. The effect of ultrasound on casein micelle integrity. J. Dairy Sci. 95:6882–6890. https://doi.org/10.3168/jds.2012-5318.

Deeth, H. C., and J. Hartanto. 2009. Chemistry of milk: Role of constituents in evaporation and drying. Pages 1–27 in Dairy Powders and Concentrated Products. A. Y. Tamime, ed. Wiley-Blackwell.

Deng, X., and R. N. Davé. 2017. Breakage of fractal agglomerates. Chem. Eng. Sci. 161:117–126. https://doi.org/10.1016/j.ces.2016.12.018.

Er, B., D. Sert, and E. Mercan. 2019. Production of skim milk powder by spray-drying from transglutaminase treated milk concentrates: Effects on physicochemical, powder flow, thermal and microstructural characteristics. Int. Dairy J. 99:104544. https://doi.org/10.1016/j.idairyj.2019.104544.

Foerster, M., T. Gengenbach, M. W. Woo, and C. Selomulya. 2016. The impact of atomization on the surface composition of spray-dried milk droplets. Colloids Surf. B Biointerfaces 140:460–471. https://doi.org/10.1016/j.colsurfb.2016.01.012.

Gaiani, C., M. Morand, C. Sanchez, E. A. Tehrany, M. Jacquot, P. Schuck, R. Jeantet, and J. Scher. 2010. How surface composition of high milk proteins powders is influenced by spray-drying temperature. Colloids Surf. B Biointerfaces 75:377–384. https://doi.org/10.1016/j.colsurfb.2009.09.016.

Goalard, C., A. Samimi, L. Galet, J. A. Dodds, and M. Ghadiri. 2006. Characterization of the dispersion behavior of powders in liquids. Part. Part. Syst. Charact. 23:154–158. https://doi.org/10.1002/ppsc.200601024.

Goder, D., H. Kalman, and A. Ullmann. 2002. Fatigue characteristics of granular materials. Powder Technol. 122:19–25. https://doi.org/10.1016/S0032-5910(01)00390-4.

Golchert, D., R. Moreno, M. Ghadiri, and J. Litster. 2004. Effect of granule morphology on breakage behaviour during compression. Powder Technol. 143–144:84–96. https://doi.org/10.1016/j.powtec.2004.04.032.

Han, J., J. Fitzpatrick, K. Cronin, V. Maidannyk, and S. Miao. 2020. Breakage of infant milk formula through three different processing methods and its influence on powder properties. J. Food Eng. 282:109997. https://doi.org/10.1016/j.jfoodeng.2020.109997.

Han, J., J. Fitzpatrick, K. Cronin, V. Maidannyk, and S. Miao. 2021a. Particle size, powder properties and the breakage behaviour of infant milk formula. J. Food Eng. 292:110367. https://doi.org/10.1016/j.jfoodeng.2020.110367.

Han, J., J. Fitzpatrick, K. Cronin, and S. Miao. 2021b. Dairy powder breakage: Mechanisms, characterization methods, impacted properties and influencing factors. Trends Food Sci. Technol. 114:608–624. https://doi.org/10.1016/j.tifs.2021.05.043.

Han, J., J. Fitzpatrick, K. Cronin, and S. Miao. 2021c. Investigation of the influence of powder characteristics on the breakage of dairy powders. Food Res. Int. 150:110775 https://doi.org/10.1016/j.foodres.2021.110775.

Han, J., J. Fitzpatrick, K. Cronin, and S. Miao. 2021d. Properties of initial and broken (PC4) WPI/lactose model powders [Data set]. Zenodo. https://doi.org/10.5281/zenodo.5573837.

Han, J., J. Fitzpatrick, K. Cronin, and S. Miao. 2022. Effects of different breakage mechanisms on the physical, water sorption, and mechanical characteristics of infant milk formula. J. Food Eng. 321:110939. https://doi.org/10.1016/j.jfoodeng.2022.110939.

Hanley, K. J. 2011. Experimental quantification and modelling of attrition of infant formulae. PhD Thesis. Department of Process and Chemical Engineering, University College Cork, Ireland.

Hanley, K. J., K. Cronin, C. O'Sullivan, M. A. Fenelon, J. A. O'Mahony, and E. P. Byrne. 2011. Effect of composition on the mechanical response of agglomerates of infant formulae. J. Food Eng. 107:71–79. https://doi.org/10.1016/j.jfoodeng.2011.05.042.

Hazlett, R., C. Schmidmeier, and J. A. O'Mahony. 2020. Influence of mechanical integrity during pneumatic conveying on the bulk handling and rehydration properties of agglomerated dairy powders. J. Food Eng. 288:110103. https://doi.org/10.1016/j.jfoodeng.2020.110103.

Ji, J., K. Cronin, J. Fitzpatrick, M. Fenelon, and S. Miao. 2015. Effects of fluid bed agglomeration on the structure modification and reconstitution behaviour of milk protein isolate powders. J. Food Eng. 167:175–182. https://doi.org/10.1016/j.jfoodeng.2015.01.012.

Ji, J., J. Fitzpatrick, K. Cronin, A. Crean, and S. Miao. 2016. Assessment of measurement characteristics for rehydration of milk protein based powders. Food Hydrocoll. 54:151–161. https://doi.org/10.1016/j.foodhyd.2015.09.027.

Kalman, H. 1999. Attrition control by pneumatic conveying. Powder Technol. 104:214–220. https://doi.org/10.1016/S0032-5910(99)00097-2.

Kalman, H. 2000. Attrition of powders and granules at various bends during pneumatic conveying. Powder Technol. 112:244–250. https://doi.org/10.1016/S0032-5910(00)00298-9.

Kim, E. H. J., X. Chen, and D. Pearce. 2005. Effect of surface composition on the flowability of industrial spray-dried dairy powders. Colloids Surf. B Biointerfaces 46:182–187. https://doi.org/10.1016/j.colsurfb.2005.11.005.

Kim, E. H. J., X. D. Chen, and D. Pearce. 2009. Surface composition of industrial spray-dried milk powders. 2. Effects of spray drying conditions on the surface composition. J. Food Eng. 94:169–181. https://doi.org/10.1016/j.jfoodeng.2008.10.020.

Kim, E. H. J., X. Dong Chen, and D. Pearce. 2003. On the mechanisms of surface formation and the surface compositions of industrial milk powders. Dry. Technol. 21:265–278. https://doi.org/10.1081/DRT-120017747.

Konami, M., S. Tanaka, and K. Matsumoto. 2002. Attrition of granules during repeated pneumatic transport. Powder Technol. 125:82–88. https://doi.org/10.1016/S0032-5910(02)00002-5.

Kotzur, B. A., R. J. Berry, S. Zigan, P. García-Triñanes, and M. S. A. Bradley. 2018. Particle attrition mechanisms, their characterisation, and application to horizontal lean phase pneumatic conveying systems: A review. Powder Technol. 334:76–105. https://doi.org/10.1016/j.powtec.2018.04.047.

Li, R., Y. H. Roos, and S. Miao. 2016a. The effect of water plasticization and lactose content on flow properties of dairy model solids. J. Food Eng. 170:50–57. https://doi.org/10.1016/j.jfoodeng.2015.09.014.

Li, R., Y. H. Roos, and S. Miao. 2016b. Flavor release from spray-dried amorphous matrix: Effect of lactose content and water plasticization. Food Res. Int. 86:147–155. https://doi.org/10.1016/j.foodres.2016.06.003.

Li, R., Y. H. Roos, and S. Miao. 2016c. Roles of particle size on physical and mechanical properties of dairy model solids. J. Food Eng. 173:69–75. https://doi.org/10.1016/j.jfoodeng.2015.10.041.

Liu, L., K. D. Kafui, and C. Thornton. 2010. Impact breakage of spherical, cuboidal and cylindrical agglomerates. Powder Technol. 199:189–196. https://doi.org/10.1016/j.powtec.2010.01.007.

Lu, X., C. Liu, L. Zhu, and X. Qu. 2014. Influence of process parameters on the characteristics of TiAl alloyed powders by fluidized bed jet milling. Powder Technol. 254:235–240. https://doi.org/10.1016/j.powtec.2013.11.013.

Maidannyk, V., D. J. McSweeney, S. A. Hogan, S. Miao, S. Montgomery, M. A. E. Auty, and N. A. McCarthy. 2020. Water sorption and hydration in spray-dried milk protein powders: Selected physicochemical properties. Food Chem. 304:125418. https://doi.org/10.1016/j.foodchem.2019.125418.

McCarthy, N. A., V. L. Gee, D. K. Hickey, A. L. Kelly, J. A. O'Mahony, and M. A. Fenelon. 2013. Effect of protein content on the physical stability and microstructure of a model infant formula. Int. Dairy J. 29:53–59. https://doi.org/10.1016/j.idairyj.2012.10.004.

Murrieta-Pazos, I., C. Gaiani, L. Galet, B. Cuq, S. Desobry, and J. Scher. 2011. Comparative study of particle structure evolution during water sorption: Skim and whole milk powders. Colloids Surf. B Biointerfaces 87:1–10. https://doi.org/10.1016/j.colsurfb.2011.05.001.

GEA Niro. 2006. GEA Niro analytical methods dry products. GEA Process Engineering A/S.

Norazirah, A., S. H. S. Fuad, and M. H. M. Hazizan. 2016. The effect of size and shape on breakage characteristic of mineral. Procedia Chem. 19:702–708. https://doi.org/10.1016/j.proche.2016.03.073.

Petukhov, Y., and H. Kalman. 2004. Empirical breakage ratio of particles due to impact. Powder Technol. 143–144:160–169. https://doi.org/10.1016/j.powtec.2004.04.009.

Rennie, P. R., X. Chen, C. Hargreaves, and A. R. Mackereth. 1999. A study of the cohesion of dairy powders. J. Food Eng. 39:277–284. https://doi.org/10.1016/S0260-8774(98)00158-7.

Reynolds, G. K., J. S. Fu, Y. S. Cheong, M. J. Hounslow, and A. D. Salman. 2005. Breakage in granulation: A review. Chem. Eng. Sci. 60:3969–3992. https://doi.org/10.1016/j.ces.2005.02.029.

Samimi, A., M. Ghadiri, R. Boerefijn, A. Groot, and R. Kohlus. 2003. Effect of structural characteristics on impact breakage of agglomerates. Powder Technol. 130:428–435. https://doi.org/10.1016/S0032-5910(02)00246-2.

Sert, D., and E. Mercan. 2021. Assessment of powder flow, functional and microbiological characteristics of ozone-treated skim milk powder. Int. Dairy J. 121:105121. https://doi.org/10.1016/j.idairyj.2021.105121.

Sert, D., E. Mercan, M. Dinkul, and S. Aydemir. 2021. Processing of skim milk powder made using sonicated milk concentrates: A study of physicochemical, functional, powder flow and microbiological characteristics. Int. Dairy J. 120:105080. https://doi.org/10.1016/j.idairyj.2021.105080.

Shrestha, A. K., T. Howes, B. P. Adhikari, B. J. Wood, and B. R. Bhandari. 2007. Effect of protein concentration on the surface composition, water sorption and glass transition temperature of spray-dried skim milk powders. Food Chem. 104:1436–1444. https://doi.org/10.1016/j.foodchem.2007.02.015.

Yan, H., and G. V. Barbosa-Cánovas. 1997. Características de la compresión de alimentos en polvo: Efecto del tamaño del aglomerado y del contenido de humedad [Compression characteristics of agglomerated food powders: Effect of agglomerate size and water activity]. Food Sci. Technol. Int. 3:351–359. https://doi.org/10.1177/108201329700300506.

Yan, H., and G. V. Barbosa-Cánovas. 2001a. Attrition evaluation for selected agglomerated food powders: The effect of agglomerate size and water activity. J. Food Process Eng. 24:37–49. https://doi.org/10.1111/j.1745-4530.2001.tb00530.x.

Yan, H., and G. V. Barbosa-Cánovas. 2001b. The effect of padding foam on the compression characteristics of some agglomerated food powders. Food Sci. Technol. Int. 7:417–423. https://doi.org/10.1106/WC69-QFNV-VN6E-LH00.

Zhang, F., A. K. Olaleye, J. A. O'Mahony, S. Miao, and K. Cronin. 2020. Dilute phase pneumatic conveying of whey protein isolate powders: Particle breakage and its effects on bulk properties. Adv. Powder Technol. 31:3342–3350. https://doi.org/10.1016/j.apt.2020.06.019.

ORCIDS

Jie Han https://orcid.org/0000-0001-6308-8052
Song Miao https://orcid.org/0000-0002-8385-3513